

Anisotropy of spin-orbit induced electron spin relaxation in [001] and [111] grown GaAs quantum dots

C. Segarra, J. Planelles,* J. I. Climente, and F. Rajadell

Departament de Química Física i Analítica, Universitat Jaume I, Castelló de la Plana, Spain

(Dated: September 9, 2014)

We report a systematic study of the spin relaxation anisotropy between single electron Zeeman sublevels in cuboidal GaAs quantum dots (QDs). The QDs are subject to an in-plane magnetic field. As the field orientation varies, the relaxation rate oscillates periodically, showing “magic” angles where the relaxation rate is suppressed by several orders of magnitude. This behavior is found in QDs with different shapes, heights, crystallographic orientations and external fields. The origin of these angles can be traced back to the symmetries of the spin admixing terms of the Hamiltonian. In [001] grown QDs, the suppression angles are different for Rashba and Dresselhaus spin-orbit terms. By contrast, in [111] grown QDs they are the same, which should facilitate a thorough suppression of spin-orbit induced relaxation. Our results evidence that cubic Dresselhaus terms play a critical role in determining the spin relaxation anisotropy even in quasi-2D QDs.

PACS numbers: 73.21.La, 72.25.Rb, 71.70.Ej

Keywords: Spin-orbit interaction, Spin relaxation, Quantum dot, Magnetic field

I. INTRODUCTION

The electron spin confined in semiconductor QDs is a promising candidate for the realization of quantum computing and the development of spin-based devices in spintronics.^{1,2} Using the spin of electrons as qubits was first proposed by Loss and DiVincenzo (Ref. 3) and, since then, a lot of effort has been devoted to its accomplishment.⁴ QDs offer the possibility of isolating single electron spins which exhibit longer lifetimes than in delocalized systems since quantum confinement suppresses the main bulk decoherence mechanisms.⁵ Nevertheless, coupling between the electron spin and the surrounding environment cannot be avoided, resulting in spin relaxation and decoherence. Therefore, a good understanding of the relaxation mechanisms in QDs is needed for the development of spin-based applications.

The two main mechanisms of spin relaxation in III-V zinc-blende semiconductor QDs are the hyperfine coupling with the nuclear spins of the lattice and the spin-orbit interaction (SOI).⁴ The hyperfine interaction is generally important at relatively weak magnetic fields while for moderate and strong fields the phonon-mediated relaxation due to SOI predominates. In semiconductors without inversion symmetry, e.g. GaAs, SOI can be originated by the bulk inversion asymmetry of the material (Dresselhaus SOI)⁶ and the structure inversion asymmetry of the confining potential (Rashba SOI).⁷ The Hamiltonians describing both SOI have different symmetries and exhibit an anisotropic behavior.⁸ This anisotropy can be exploited to externally control and manipulate the electron spin by changing the orientation of applied magnetic or electric fields.^{9–11} As a consequence, the anisotropy of the spin relaxation and its control via external means has been intensively studied.^{12–17}

Most works so far have dealt with two-dimensional (2D) parabolic InAs or GaAs QDs grown along the [001] crystal direction,^{4,12–14} where in-plane anisotropy arises

from the interference between Rashba and Dresselhaus SOI. However, realistic QDs are prone to deviate from the circular symmetry and there is gathering evidence that this has a primary influence on the spin relaxation anisotropy.^{15–17} Yet, previous works on this aspect neglected cubic Dresselhaus SOI terms, whose role may be important. Cubic terms are expected to become particularly important in QDs with large height-to-base aspect ratio¹⁸, which are increasingly available owing to recent progress in synthetic control.^{19,20} Going beyond [001] grown QDs is also of interest, especially in view of the convenience of [111] grown QDs for optical spin preparation.²¹ The effect of the crystallographic orientation on the spin dynamics has been well studied in quantum wells^{22–24}, but further work is needed in relation to fully localized spins.

In this work, we study the anisotropy of the electron spin relaxation between Zeeman sublevels in cuboidal GaAs QDs. The anisotropy is monitored by varying the orientation of an externally applied in-plane magnetic field (ϕ_B). We consider QDs grown along both [001] and [111] crystal directions, including all linear and cubic terms of Rashba and Dresselhaus SOI in a fully 3D model. Different heights, base shapes, crystallographic orientations and external electric fields are considered. The numerical results, together with perturbative interpretations, provide a wide overview on the effect of confinement asymmetry and three-dimensionality on the spin relaxation anisotropy.

We find that, in [001] grown QDs, the spin relaxation anisotropy is very different depending on the dominating spin-orbit mechanism, Rashba or Dresselhaus SOI. By contrast, in [111] grown QDs the anisotropy is the same for both terms. In all cases, the spin relaxation rate shows strong oscillations with ϕ_B . Interestingly, cubic Dresselhaus terms are shown to be critical in determining such anisotropic behavior. This occurs not only in high QDs, but – contrary to common belief – also in quasi-

2D QDs, provided the high symmetry directions of the dot are not aligned with the main crystallographic axes. In both squared and rectangular QDs we observe order-of-magnitude suppressions of the spin relaxation rate at certain “magic” magnetic field angles ϕ_B , which can be understood from symmetry considerations.

The paper is organized as follows. Sec. II presents the model we use to compute the electron spin relaxation, including the SOI Hamiltonians for QDs rotated with respect to the main crystallographic axes. In Sec. III we show and discuss the numerical results for the cases under study. Finally, conclusions are given in Sec. IV.

II. THEORETICAL MODEL

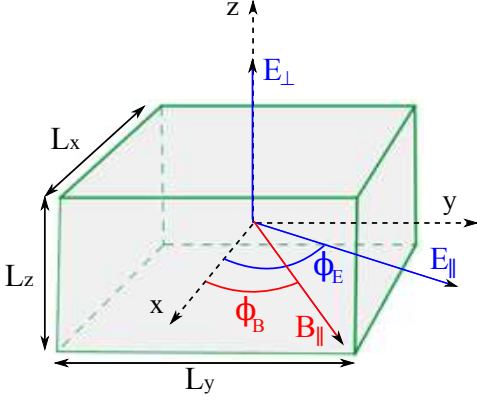


FIG. 1: Schematic representation of the cuboidal QD system. The orientation of the external electric and magnetic fields is indicated.

We study the electron spin relaxation driven by SOI between Zeeman split sublevels of cuboidal GaAs QDs subject to externally applied electric \mathbf{E} and magnetic \mathbf{B} fields (see Fig. 1). The one-electron states are described by a three-dimensional Hamiltonian of the form

$$H = \frac{\mathbf{p}^2}{2m^*} + V_c + \mathbf{E}\mathbf{r} + H_Z + H_{SOI}, \quad (1)$$

where m^* stands for the electron effective mass, V_c is the confinement potential, \mathbf{E} is an external electric field and $\mathbf{p} = -i\hbar\nabla + \mathbf{A}$, where \mathbf{A} is the vector potential. An in-plane magnetic field $\mathbf{B} = B(\cos\phi_B, \sin\phi_B, 0)$ rotated an angle ϕ_B with respect to the x axis of the dot is included. This field is described by the vector potential $\mathbf{A} = (zB\sin\phi_B, -zB\cos\phi_B, 0)$. The Zeeman term is $H_Z = \frac{1}{2}g\mu_B\mathbf{B}\boldsymbol{\sigma}$ with g , μ_B and $\boldsymbol{\sigma}$ standing for the electron g -factor, Bohr magneton and Pauli spin matrices, respectively.

The last term in Eq. (1) corresponds to the SOI,⁸ $H_{SOI} = H_R + H_D$, with H_R being the Rashba SOI

$$H_R^{[001]} = r\boldsymbol{\sigma}(\mathbf{p} \times \mathbf{E}), \quad (2)$$

and H_D the Dresselhaus SOI

$$H_D^{[001]} = d[\sigma_x p_x (p_y^2 - p_z^2) + \sigma_y p_y (p_z^2 - p_x^2) + \sigma_z p_z (p_x^2 - p_y^2)] \quad (3)$$

Here, r and d are material-dependent coefficients determining the strength of the SOI and the superscript [001] indicates the growth direction of the QD.

Eq. (2) and Eq. (3) correspond to QDs grown along the [001] crystal direction. In order to consider other orientations of the QD with respect to the crystal host we maintain the confinement potential fixed in space and perform a rotation of the crystalline structure. Since the confining potential as well as the externally applied fields are kept while the crystalline structure is rotated, only the H_{SOI} part of the Hamiltonian is affected. In particular, the H_{SOI} Hamiltonian corresponding to an axially applied electric field and a crystalline structure subject to an in-plane rotation θ_z around the z axis read:

$$H_R^{[001]}(\theta_z) = rE_z(\sigma_x p_y - \sigma_y p_x), \quad (4)$$

and

$$H_D^{[001]}(\theta_z) = d \cos 2\theta_z [\sigma_x p_x (p_y^2 - p_z^2) + \sigma_y p_y (p_z^2 - p_x^2) + \sigma_z p_z (p_x^2 - p_y^2)] + d \sin 2\theta_z [p_z^2 (\sigma_y p_x + \sigma_x p_y) - 2\sigma_z p_x p_y p_z + \frac{1}{2}(p_x^2 - p_y^2)(\sigma_x p_y - \sigma_y p_x)]. \quad (5)$$

Note that this particular case of an axially applied electric field yields a Rashba Hamiltonian (4) independent of θ_z .

We consider next QDs grown along the [111] direction. In particular, we consider the rotation $\chi = \arccos(1/\sqrt{3})$ around the straight line $y = -x$, that correspond to the Euler angles $\theta = \arccos(1/\sqrt{3})$, $\phi = 45$ and $\alpha = -45$. The rotated SOI Hamiltonians have the form

$$H_R^{[111]} = \frac{rE_z}{\sqrt{3}} [\sigma_z(p_y - p_x) - \sigma_y(p_x + p_z) + \sigma_x(p_y + p_z)], \quad (6)$$

and

$$H_D^{[111]} = \frac{d}{2\sqrt{3}} [(p_x^2 + p_y^2 - 4p_z^2)(p_x\sigma_y - p_y\sigma_x) + p_z(p_x^2 - p_y^2)(\sigma_x + \sigma_y) + 2p_x p_y p_z(\sigma_x - \sigma_y) - \sigma_z p_x^2(p_x + 3p_y) + \sigma_z p_y^2(p_y + 3p_x)], \quad (7)$$

where the electric field is aligned with the dot z axis.

The relaxation rate between the initial electron state $|\Psi_i\rangle$ and the final electron state $|\Psi_f\rangle$ is estimated by the Fermi golden rule

$$\frac{1}{T_1} = \frac{2\pi}{\hbar} \sum_{\lambda, \mathbf{q}} |M_\lambda(\mathbf{q})|^2 |\langle \Psi_f | e^{-i\mathbf{q}\mathbf{r}} | \Psi_i \rangle|^2 \delta(E_f - E_i - E_q) \quad (8)$$

Here, \mathbf{q} is the bulk phonon wave vector and $M_\lambda(\mathbf{q})$ denotes the scattering matrix element corresponding to the

electron-phonon interaction λ , being the piezoelectric or the deformation potentials.²⁵ All calculations are carried out at zero temperature, thus only phonon emission processes are possible. The splitting energy between Zeeman sublevels is small so that only acoustic phonons are important and the linear dispersion regime applies $E_q = \hbar c_\alpha q$, where c_α is the sound velocity of the longitudinal or transversal phonon branch.²⁶ Note that phonons cannot couple states with opposite spin and the spin admixture caused by SOI is essential for relaxation to take place.

The eigenvalue problem is solved numerically using a finite difference method on a three-dimensional grid. Accounting for SOI in the calculation of the energy spectra requires high numerical precision due to the small magnitude of this coupling and the presence of third-order derivatives. Different approaches to approximate the derivatives in the finite difference method have been studied. After a series of convergence tests, a 7-point stencil central difference scheme and a number of 42875 mesh nodes discretizing the 3D system has been employed in all calculations yielding matrices of dimensions 85750x85750. With this, we guarantee an accurate description of the electron states at a reasonable computational cost.

The QD system is described with a hard-wall confinement potential. We use GaAs material parameters, particularly electron effective mass $m^* = 0.067$, density $\rho = 5310 \text{ kg/m}^3$, dielectric constant $\epsilon_r = 12.9$, piezoelectric constant $h_{14} = 1.45 \cdot 10^9 \text{ V/m}$, g-factor $g = -0.44$ and sound velocities $c_l = 4720 \text{ m/s}$ and $c_t = 3340 \text{ m/s}$.^{22,28} For the SOI constants, we take $d = 27.58 \text{ eV}\text{\AA}^3$ and $r = 5.026 \text{ e}\text{\AA}^2$.⁸ All simulations are carried out, unless otherwise stated, considering an axial electric field $E_z = 10 \text{ kV/cm}$ and an in-plane magnetic field $B_{\parallel} = 1T$.

III. RESULTS AND DISCUSSION

A. Geometry dependence

We investigate first the relaxation rate anisotropy for different dot geometries when applying an in-plane magnetic field at different orientations. The QDs considered have a base with square ($L_x = 80 \text{ nm}$, $L_y = 80 \text{ nm}$) or rectangular ($L_x = 70 \text{ nm}$, $L_y = 90 \text{ nm}$) shape and various heights ranging from $L_z = 10 \text{ nm}$ to $L_z = 40 \text{ nm}$.

Fig. 2 shows the spin relaxation rate when only Rashba SOI is present. For QDs with square base the relaxation rate is the same regardless of ϕ_B . In contrast, in rectangular QDs it presents an anisotropic behavior, where the maximum (minimum) corresponds to a magnetic field oriented along the direction of weaker (stronger) confinement. In both cases, $1/T_1$ is independent of the QD height and, for the sake of clarity, only results for $L_z = 10 \text{ nm}$ are included in Fig. 2.

In Fig. 3(a), we analyze the spin relaxation in the only presence of Dresselhaus SOI for QDs with square

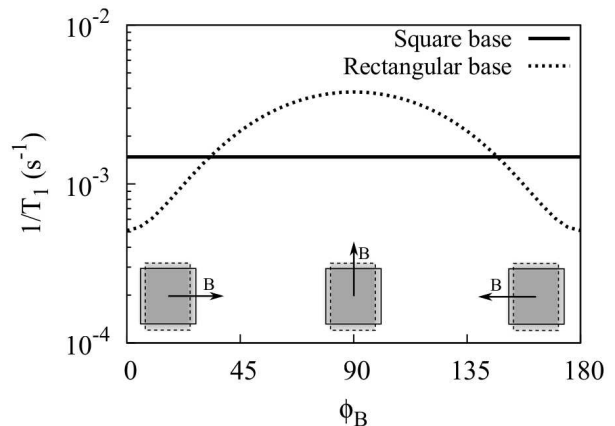


FIG. 2: Electron spin relaxation rate as a function of the in-plane magnetic field orientation when only the Rashba SOI contribution is included. QDs of 10nm height with rectangular (dotted line) and square base (solid line) are considered.

base. The relaxation rate for small QDs ($L_z = 10 \text{ nm}$) is almost isotropic with the orientation of the magnetic field. This is in sharp contrast with higher QDs, where strong quenchedings are found at $\phi_B = 45$ and $\phi_B = 135$. On the other hand, when the QD base is rectangular, Fig. 3(b), only moderate modulations of $1/T_1$ are observed. Again, the dependence on ϕ_B is different depending on the dot height. When B_{\parallel} is oriented along the direction of weaker confinement the relaxation is minimum for QDs with $L_z = 10 \text{ nm}$, but it changes into a maximum for $L_z = 20, 30, 40 \text{ nm}$.

The preceding results reveal a strong sensitivity of the spin relaxation anisotropy to both the QD symmetry (squared or rectangular) and the QD height. Both factors can induce major, qualitative changes in the anisotropy. To understand such a behavior, we consider that the relaxation rate is proportional to the degree of spin admixture of the initial and final states of the transition, Ψ_i and Ψ_f in Eq. (8).²⁶ These states can be approximated as:

$$\begin{aligned} \Psi_i &\approx \psi_{000}|\downarrow\rangle + c_x^i \psi_{100}|\uparrow\rangle + c_y^i \psi_{010}|\uparrow\rangle \\ \Psi_f &\approx \psi_{000}|\uparrow\rangle + c_x^f \psi_{100}|\downarrow\rangle + c_y^f \psi_{010}|\downarrow\rangle \end{aligned} \quad (9)$$

where ψ_{ijk} represents the electron orbital in the absence of SOI, with ijk the number of nodes in x , y and z , respectively, while $|\uparrow\rangle$ ($|\downarrow\rangle$) represents parallel (antiparallel) spin alignment along the direction of the magnetic field. For the analysis we can focus on Ψ_i (analogous reasoning is valid for Ψ_f). Ψ_i is mostly a spin down state, with a little SOI induced spin admixture with excited levels. Notice that $\psi_{000}|\uparrow\rangle$ does not contribute to the spin admixture of Ψ_i because the parity symmetry in x and y prevents direct SOI coupling with $\psi_{000}|\downarrow\rangle$. Thus, the degree of spin admixture is essentially captured by the coefficients c_x^i and c_y^i , which can be estimated per-

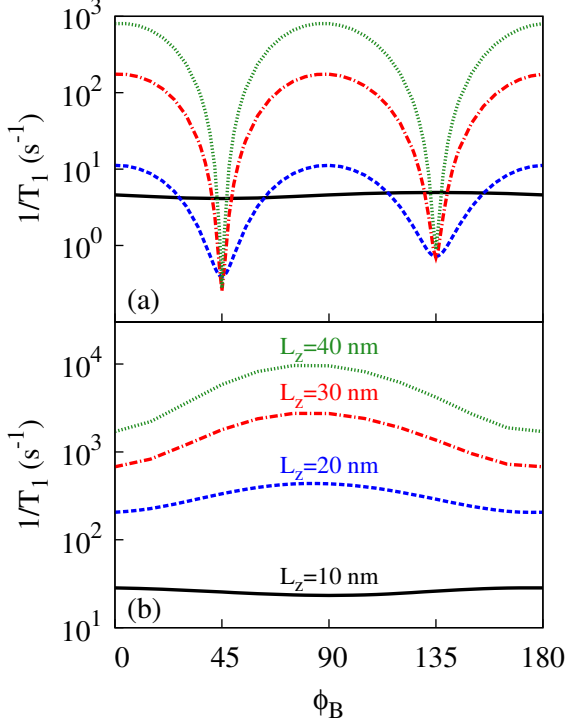


FIG. 3: Calculated spin relaxation rate vs. magnetic field orientation ϕ_B considering only Dresselhaus SOI in (a) square and (b) rectangular base QDs. Different dot heights are studied: $L_z = 10$ nm (solid black line), $L_z = 20$ nm (blue dashed line), $L_z = 30$ nm (red dash-dotted line) and $L_z = 40$ nm (green dotted line).

turbatively as:

$$c_x^i = -\frac{\langle \uparrow | \langle \psi_{100} | H_{SOI} | \psi_{000} \rangle | \downarrow \rangle}{\varepsilon_{100\uparrow} - \varepsilon_{000\downarrow}}, \quad (10)$$

and

$$c_y^i = -\frac{\langle \uparrow | \langle \psi_{010} | H_{SOI} | \psi_{000} \rangle | \downarrow \rangle}{\varepsilon_{010\uparrow} - \varepsilon_{000\downarrow}}. \quad (11)$$

The energy separations $\Delta\varepsilon_x = \varepsilon_{100\uparrow} - \varepsilon_{000\downarrow}$ and $\Delta\varepsilon_y = \varepsilon_{010\uparrow} - \varepsilon_{000\downarrow}$ do not vary with ϕ_B . Thus, the origin of the anisotropy must be sought in the SOI matrix elements.

We consider first Rashba SOI, i.e. $H_{SOI} = H_R^{[001]}(0)$. From Eq. (4) and parity considerations, it follows that, for $\phi_B = 0$,

$$c_x^i = r E_z \frac{\langle \uparrow | \sigma_y | \downarrow \rangle \langle \psi_{100} | p_x | \psi_{000} \rangle}{\Delta\varepsilon_x}, \quad c_y^i = 0 \quad (12)$$

while for $\phi_B = 90$,

$$c_x^i = 0, \quad c_y^i = r E_z \frac{\langle \uparrow | \sigma_x | \downarrow \rangle \langle \psi_{010} | p_y | \psi_{000} \rangle}{\Delta\varepsilon_y}. \quad (13)$$

We see that depending on the orientation of the magnetic field the spin admixture is caused by the coupling to a

different excited state. For QDs with square base $\Delta\varepsilon_x = \Delta\varepsilon_y$, and $\langle \psi_{100} | p_x | \psi_{000} \rangle = \langle \psi_{010} | p_y | \psi_{000} \rangle$. Consequently, the degree of spin mixing does not change at $\phi_B = 0$ and $\phi_B = 90$, in agreement with the isotropic $1/T_1$ observed in Fig. 2. Conversely, in rectangular QDs with stronger confinement in x , $\Delta\varepsilon_x > \Delta\varepsilon_y$. Then, the admixture coefficients at $\phi_B = 90$ are larger than at $\phi_B = 0$, which justifies the anisotropy observed in Fig. 2.

The anisotropy of Dresselhaus SOI induced spin relaxation, shown in Fig. 3, can be understood in similar terms. We split Eq. (3) as $H_D^{[001]} = H_z + H_{xy}$, where $H_z = d p_z^2 (p_y \sigma_y - p_x \sigma_x)$ and $H_{xy} = H_x + H_y = d [p_x^2 (p_z \sigma_z - p_y \sigma_y) + p_y^2 (p_x \sigma_x - p_z \sigma_z)]$. Calculations using these Hamiltonians independently show that H_z dominates for $L_z = 10$ nm, in agreement with the usual practice of approximating the Dresselhaus SOI by H_z in quasi-2D systems. If we perform a similar analysis for H_z as the one carried out for Rashba SOI, we find that coupling to ψ_{010} and ψ_{100} dominates at $\phi_B = 0$ and $\phi_B = 90$, respectively. This is exactly the opposite as for the Rashba SOI case, explaining the results obtained for $L_z = 10$ nm QDs (see Fig. 3(b)). As the QD height is increased, however, H_{xy} soon dominates over H_z . Indeed, for $L_z = 20$ nm it is already dominant. Considering individually H_x and H_y it can be shown that they present opposite behaviors with ϕ_B . H_x produces a maximum (minimum) relaxation for $\phi_B = 90$ ($\phi_B = 0$) and H_y for $\phi_B = 0$ ($\phi_B = 90$). This dependence does not change with the base shape and a stronger confinement in one direction only determines which term, H_x or H_y , prevails. In the rectangular dot of Fig. 3(b), $L_x < L_y$ so H_x is more important and we observe its angular dependence. Instead, when the dot base is squared H_x and H_y cancel each other out at $\phi_B = 45$ and $\phi_B = 135$, thus giving rise to the pronounced minima of $1/T_1$ observed in Fig. 3(a).

To summarize this section, the spin relaxation anisotropy of [001] grown GaAs QDs is determined by the spin admixture induced by SOI. This is qualitatively different in systems where Rashba or Dresselhaus SOI terms dominate. In the latter case, the anisotropy reflects whether H_z or H_{xy} prevails. It turns out that H_{xy} is already dominant for $L_z = 20$ nm (height-to-base aspect ratio of 1:4), which points out at the early relevance of cubic Dresselhaus terms in structures where three-dimensionality starts becoming important. In this case, the use of QDs with symmetric x-y confinement enables strong suppressions of the relaxation at certain magnetic field orientations. These “magic” angles are reminiscent of the “easy passages” found by Stano and Fabian for laterally coupled circular QDs.¹⁴ In this and the following sections we show that related physics arises for single QDs with non-circular confinement, which has significant practical implications.

B. In-plane confinement potential orientation

In this section, we investigate the impact of the QD orientation with respect to the crystal host on the spin relaxation. The rotation angle θ_z is defined as the angle between the [001] crystal direction and the x axis of the dot, see inset of Fig. 4 for a schematic representation. All calculations are carried out with the magnetic field $B_{\parallel} = 1$ T oriented along the x axis of the QD and an axial electric field $E_z = 10$ kV/cm.

In Fig. 4(a), we plot the relaxation rate in the presence of Rashba SOI only for QDs with $L_z = 10$ nm (results for $L_z = 20$ nm are identical and are omitted for clarity). We find that $1/T_1$ is not affected by changes in the dot orientation. This result is as expected since Eq. (4) does not depend on θ_z .

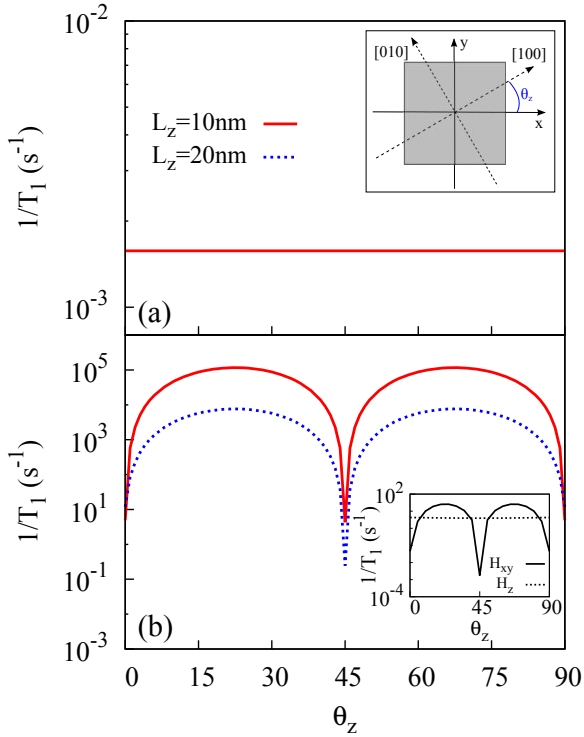


FIG. 4: Spin relaxation rate as a function of the dot orientation θ_z for square base QDs with $L_z = 10$ nm (black solid curve) and $L_z = 20$ nm (blue dotted curve). Results are shown for (a) pure Rashba SOI and (b) pure Dresselhaus SOI. The in-plane magnetic field $B_{\parallel} = 1$ T is oriented along the dot x axis ($\phi_B = 0$). The inset in (a) illustrates a representation of the system and the definition of the rotation angle. The inset in (b) shows the relaxation due to H_{xy} and H_z in the $L_z = 10$ nm dot.

For the Dresselhaus SOI case instead, Fig. 4(b) shows a strong dependence of $1/T_1$ on the confinement potential rotation. In particular, one can see some specific rotation angles, $\theta_z = 0, 45, 90$, where the spin relaxation is reduced by 4-5 orders of magnitude as compared to others. This behavior can be understood from the form of the

Hamiltonian in Eq. (5). The Dresselhaus SOI presents a $2\theta_z$ dependence, with half of the terms multiplied by $\sin 2\theta_z$ and the other half by $\cos 2\theta_z$. Therefore, the first part of Eq. (5) cancels for $\theta_z = 45$ and the second part for $\theta_z = 0$ and $\theta_z = 90$. This suppresses some of the SOI coupling channels, giving rise to slower relaxation rate than for intermediate angles.

It is noteworthy to mention that the dependence on θ_z originates in H_{xy} , with H_z remaining isotropic, see Fig. 4(b) inset. This highlights the important role of the cubic terms of the Dresselhaus SOI Hamiltonian in GaAs QDs. As a matter of fact, the inset shows that even in the shortest QDs ($L_z = 10$ nm), save for the vicinity of the “magic” rotation angles ($\theta_z = 0, 45, 90$) the main contribution to the relaxation rate does not come from H_z but from H_{xy} .

These results are robust against changes in the QD geometry, such as height and base shape, which do not modify the qualitative trend. In particular, the minimum at $\theta_z = 45$ remains unaltered while the minima at $\theta_z = 0$ and $\theta_z = 90$ is slightly shifted in rectangular QDs.

C. Effect of an additional in-plane electric field

We next explore the influence of applying an in-plane electric field on the spin relaxation anisotropy. We consider the squared QD of Sec. III A with $B_{\parallel} = 1$ T and $E_z = 10$ kV/cm, but now we add an additional electric field component $E_{\parallel} = 10$ kV/cm. Calculations are performed rotating the in-plane electric field for some fixed magnetic field orientations.

In Fig. 5(a) and Fig. 5(b), we present the relaxation rate obtained for pure Rashba and pure Dresselhaus SOI, respectively, at four different ϕ_B values. The most remarkable finding is that $1/T_1$ is increased by several orders of magnitude in comparison with the case with only axial electric field (Fig. 2 and Fig. 3), although strong suppressions show up at some specific combinations of ϕ_B and ϕ_E . For Rashba SOI the combination is $\phi_B - \phi_E = 90, 270$ and for Dresselhaus SOI $\phi_B + \phi_E = 0, 180$. Changes in the QD geometry do not modify significantly the qualitative results shown in Fig. 5. Only small displacements of the cancellation angles and the moderation of some minima occur.

The influence of the in-plane electric field can be explained from the fact that E_{\parallel} breaks the parity symmetry in the direction ϕ_E . This enables the otherwise forbidden SOI coupling between the Zeeman sublevels $\psi_{000} | \uparrow \rangle$ and $\psi_{000} | \downarrow \rangle$ in Ψ_i and Ψ_f (recall Sec. III A). Since these states are very close in energy, the ensuing spin admixture is important, which justifies the large enhancement of $1/T_1$. In order to understand the minima we carry out a similar perturbative analysis to that of Sec. III A but now focusing on the coupling between the two ψ_{000} sublevels. Let us consider first the Dresselhaus SOI term. Assuming $H_D^{[001]} \approx H_z$ (as is the case for quasi-2D QDs

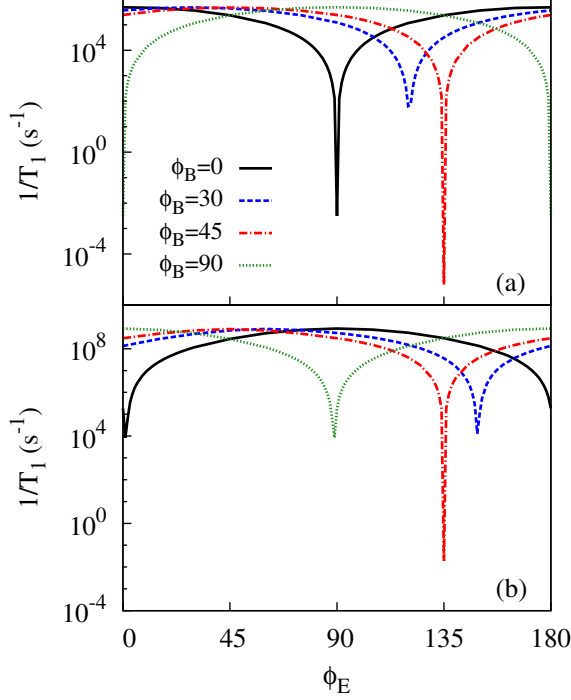


FIG. 5: Electron spin relaxation as a function of the in-plane electric field orientation ϕ_E considering (a) only Rashba SOI and (b) only Dresselhaus SOI. The QDs studied have square base and $L_z = 10$ nm. Calculations with the magnetic field oriented at some fixed angles are presented: $\phi_B = 0$ (black solid line), $\phi_B = 30$ (blue dashed line), $\phi_B = 45$ (red dash-dotted line) and $\phi_B = 90$ (green dotted line)

and $\theta_z = 0$), the $\phi_B = 0$ matrix element is:

$$\langle \psi_{000} | \uparrow | H_z | \psi_{000} | \downarrow \rangle = d \langle \downarrow | \sigma_y | \uparrow \rangle \langle \psi_{000} | p_z^2 p_y | \psi_{000} \rangle \quad (14)$$

The integral of the orbital part in Eq. (14) vanishes when $\phi_E = 0$ because of the odd parity along y , but other orientations of the electric field break the parity symmetry in the y direction and then $1/T_1$ increases, as seen in Fig. 5(b) (black line). Similar reasoning shows that for $\phi_B = 90$ the parity-induced minimum occurs at $\phi_E = 90$. For intermediate magnetic field angles, however, the minimum no longer takes place when $E_{\parallel} \parallel \mathbf{B}$. Indeed, for $\phi_B = 45$, the minimum is found at $\phi_E = 135$ ($E_{\parallel} \perp \mathbf{B}$). To explain this, it is convenient to rotate the coordinate system 45 degrees from (x, y) into (x', y') so that the x' axis is aligned with the direction of \mathbf{B} . As inferred from Eq. (5), the resulting SOI term is $H_z^{45} = dp_z^2(\sigma_{y'} p'_x + \sigma_{x'} p'_y)$ and the matrix element becomes:

$$\langle \psi_{000} | \uparrow | H_z^{45} | \psi_{000} | \downarrow \rangle = d \langle \downarrow | \sigma_{y'} | \uparrow \rangle \langle \psi_{000} | p_z^2 p'_x | \psi_{000} \rangle \quad (15)$$

This integral vanishes due to the odd parity in x' when E_{\parallel} is parallel to the y' axis, i.e. when $\phi_E = 135$ in the initial coordinate frame, in agreement with Fig. 4(b).

The minima in the presence of Rashba SOI can be explained in similar terms, but because $H_R^{[001]}$ has rotational symmetry, see Eq. (4), it does not change when rotating the coordinate system. Then, the minima always take place for $E_{\parallel} \perp \mathbf{B}$.

To summarize this section, the presence of in-plane electric fields greatly enhances spin relaxation due to the lowered orbital symmetry, but the anisotropy of both Rashba and Dresselhaus SOI makes it possible to find relative angles between E_{\parallel} and \mathbf{B} such that the relaxation is severely reduced.

D. [111] grown QDs

In Fig. 6 we plot the spin relaxation rate for the squared QD studied in Sec. IIIA, but now considering the dot is grown along the [111] crystal direction. In general, faster relaxation rates are obtained for this orientation as compared to the [001] grown QDs. Interestingly, we observe the same angular dependence for both Rashba SOI (Fig. 6(a)) and Dresselhaus SOI (Fig. 6(b)). Both mechanisms show strong suppressions at $\phi_B = 135$ and $\phi_B = 315$. However, when increasing L_z Rashba and Dresselhaus SOI mechanisms show opposite behaviors and $1/T_1$ increases and decreases, respectively. Therefore, the dot height determines which of the coupling mechanisms dominates.

The cancellation angles of the relaxation in Fig. 6 can be justified noting that the canonical momenta $p_x = -i\hbar d/dx + zB \sin \phi_B$ and $p_y = -i\hbar d/dy - zB \cos \phi_B$ have exactly the same form for $\phi_B = 135$ and $\phi_B = 315$ since $L_x = L_y$. As a result, the first term in Eq. (6) and several terms in Eq. (7) cancel out, yielding two sharp minima in the scattering rate curve.

The identical anisotropy of Rashba and Dresselhaus SOI induced spin relaxation in [111] QDs revealed by Fig. 6, which is a consequence of the formal equivalences between $H_R^{[111]}$ and $H_D^{[111]}$,²⁹ facilitates in practice the simultaneous quenching of both mechanisms. For magnetic fields where hyperfine interaction is negligible and square dots, this should lead to spin lifetimes in the range of seconds. We have further checked that changes in the QD base shape do not modify the qualitative behavior reported above, the minima being only slightly shifted for rectangular dots under Dresselhaus SOI.

IV. CONCLUSIONS

We have investigated systematically the electron spin scattering anisotropy in 3D cuboidal GaAs QDs grown along the [001] and [111] directions. We have shown that the relaxation rate can be controlled by several orders of magnitude by varying the in-plane orientation of external magnetic and electric fields.

In [001] grown QDs under an axial electric field, the spin relaxation in-plane anisotropy is strongly dependent

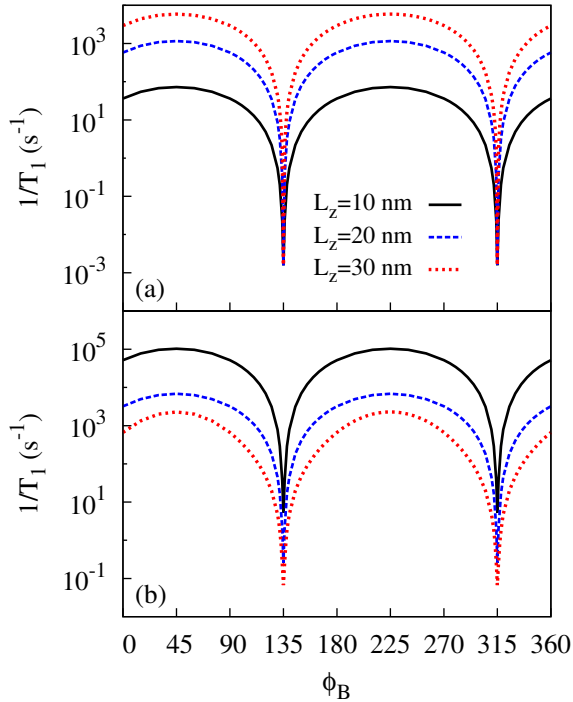


FIG. 6: Electron spin dynamics of square QDs grown along the [111] crystallographic direction as a function of the magnetic field orientation. Simulations considering (a) the Rashba SOI and (b) the Dresselhaus SOI are included for three QD heights: $L_z = 10 \text{ nm}$ (black solid curve), $L_z = 20 \text{ nm}$ (blue dashed curve) and $L_z = 30 \text{ nm}$ (red dotted curve).

on the QD geometry and the nature of the dominating SOI term. For Rashba SOI, the relaxation is isotropic or anisotropic when the base is squared and rectangu-

lar, respectively, and it is not affected by changes in the QD height. On the other hand, for Dresselhaus SOI, the relaxation presents a different behavior depending not only on the base shape, but also on the QD height. In fact, small and high dots can even show contrary angular dependence, evidencing the important role of QD three-dimensionality.

An additional in-plane electric field component causes a strong increase in the relaxation rate, but certain combinations of ϕ_B and ϕ_E lead to enhanced spin lifetimes. We find that these combinations are different for Rashba, $\phi_B - \phi_E = 90, 270$, and Dresselhaus SOI, $\phi_B + \phi_E = 0, 180$.

We have also shown that rotating the confinement potential in-plane with respect to the crystal structure causes an important modulation of the spin relaxation, that is severely suppressed when the high symmetry directions of the QD confinement match the main crystallographic axes. This modulation arises from the cubic Dresselhaus terms, which are important even for small heights.

We have further studied QDs grown along the [111] direction. We have found that Rashba and Dresselhaus SOI present the same angular dependence with ϕ_B , with pronounced minima at certain magnetic field orientations. This enables simultaneous suppression of Rashba and Dresselhaus SOI induced spin relaxation, which is an advantage as compared to more conventional [001] grown QDs.

Acknowledgments

This work was supported by UJI-Bancaixa Project No. P1-1B2011-01, MINECO Project No. CTQ2011-27324, and FPU Grant (C.S.).

-
- * Electronic address: josep.planelles@uji.es
- ¹ D. D. Awschalom, D. Loss, and N. Samarth, *Semiconductor Spintronics and Quantum Computing* (Springer, New York, 2002)
 - ² J. Fabian, A. Matos-Abiad, C. Ertler, P. Stano, and I. Žutić, *Acta Phys. Slovaca* **57**, 565 (2007)
 - ³ D. Loss and D. P. DiVincenzo, *Phys. Rev. A* **57**, 120 (1998)
 - ⁴ R. Hanson, J. R. Petta, S. Tarucha and, L. M. K. Vandersypen, *Rev. Mod. Phys.* **79**, 1217 (2007)
 - ⁵ A. V. Khaetskii and Y. V. Nazarov, *Phys. Rev. B* **61**, 12639 (2000)
 - ⁶ G. Dresselhaus, *Phys. Rev.* **100**, 580 (1955)
 - ⁷ Y. A. Bychkov and E. I. Rashba, *J. Phys. C* **17**, 6039 (1984)
 - ⁸ R. Winkler, *Spin-Orbit Coupling Effects in Two-Dimensional Electron and Hole Systems* (Springer, Berlin, 2003)
 - ⁹ J. Königsmann, R. J. Haug, D. K. Maude, V. I. Fal'ko, and B. L. Altshuler, *Phys. Rev. Lett.* **94**, 226404 (2005)
 - ¹⁰ S. Takahashi, R. S. Deacon, K. Yoshida, A. Oiwa, K. Shi-

- bata, K. Hirakawa, Y. Tokura and S. Tarucha, *Phys. Rev. Lett.* **104**, 246801 (2010)
- ¹¹ M. P. Nowak and B. Szafran, *Phys. Rev. B* **87**, 205436 (2013)
- ¹² V. I. Fal'ko, B. L. Altshuler, and O. Tsyplatyev, *Phys. Rev. Lett.* **95**, 076603 (2005)
- ¹³ C. F. Destefani, and S. E. Ulloa, *Phys. Rev. B* **72**, 115326 (2005).
- ¹⁴ P. Stano, and J. Fabian, *Phys. Rev. Lett.* **96**, 186602 (2006); *Phys. Rev. B* **74**, 045320 (2006).
- ¹⁵ O. Olendski and T. V. Shahbazyan, *Phys. Rev. B* **75**, 041306(R) (2007)
- ¹⁶ S. Amasha, K. MacLean, I. P. Radu, D. M. Zumbühl, M. A. Kastner, M. P. Hanson, and A. C. Gossard, *Phys. Rev. Lett.* **100**, 046803 (2008)
- ¹⁷ S. Prabhakar, R. Melnik, and L. L. Bonilla, *Phys. Rev. B* **87**, 235202 (2013)
- ¹⁸ J. Planelles, J. I. Climente, and C. Segarra, *J. Phys. Chem. C* **116**, 25143 (2012).
- ¹⁹ D. Dalacu, K. Mnaymneh, X. Wu, J. Lapointe, G. C. Aers,

- P. J. Poole, and R. L. Williams, Appl. Phys. Lett. **98**, 251101 (2011).
- ²⁰ A. Pfund, I. Shorubalko, R. Leturcq, and K. Ensslin, Appl. Phys. Lett. **89**, 252106 (2006).
- ²¹ T. Mano, M. Abbarchi, T. Kuroda, B. McSkimming, A. Ohtake, K. Mitsuishi, and K. Sakoda, Appl. Phys. Express **3**, 065203 (2010) and references therein.
- ²² I. Vurgaftman and J. R. Meyer, J. Appl. Phys. **97**, 053707 (2005)
- ²³ K. Biermann, A. Hernández-Mínguez, R. Hey, and P. V. Santos, J. Appl. Phys. **112**, 083913 (2012)
- ²⁴ A. Balocchi, T. Amand, G. Wang, B. L. Liu, P. Renucci, Q. H. Duong, and X. Marie, New J. Phys. **15**, 095016 (2013)
- ²⁵ J. I. Climente, A. Bertoni, G. Goldoni, and E. Molinari, Phys. Rev. B **74**, 035313 (2006)
- ²⁶ A. V. Khaetskii and Y. V. Nazarov, Phys. Rev. B **64**, 125316 (2001)
- ²⁷ I. Vurgaftman, J. R. Meyer, and L. R. Ram-Mohan, J. Appl. Phys. **89**, 5815 (2001)
- ²⁸ *Semiconductors. Physics of Group IV Elements and III-V Compounds*, edited by O. Madelung, Landolt-Börnstein, Vol. 17 (Springer-Verlag, 1982).
- ²⁹ I. Zutic, J. Fabian, and S. Das Sarma, Rev. Mod. Phys. **76**, 323 (2004).